⌘ *Author's Choice*

THE JOURNAL OF BIOLOGICAL CHEMISTRY VOL. 287, NO. 13, pp. 9731–9741, March 23, 2012

Cytochrome *b* Mutation Y268S Conferring Atovaquone Resistance Phenotype in Malaria Parasite Results in Reduced Parasite bc_1 Catalytic Turnover and Protein Expression*[S]

Received for publication, November 15, 2011, and in revised form, January 26, 2012 Published, JBC Papers in Press, January 26, 2012, DOI 10.1074/jbc.M111.324319

Nicholas Fisher[‡1], Roslaini Abd Majid[‡1,2], Thomas Antoine[‡], Mohammed Al-Helal[‡], Ashley J. Warman[‡], David J. Johnson[‡], Alexandre S. Lawrenson[§], Hilary Ranson[‡], Paul M. O'Neill[§], Stephen A. Ward[‡3], and Giancarlo A. Biagini[‡4]

From the [‡]Liverpool School of Tropical Medicine, Pembroke Place, Liverpool L3 5QA, United Kingdom and the [§]Department of Chemistry, University of Liverpool, Liverpool L69 7ZD, United Kingdom

Background: Cytochrome *b* mutations confer atovaquone resistance, resulting in antimalarial drug failures.
Results: Mutation Y268S reduces bc_1 catalytic turnover and stability.
Conclusion: Reduction of catalytic turnover and iron-sulfur protein content in parasite Y268S bc_1 confers a fitness cost. These results were not predicted using yeast models.
Significance: Data will aid novel bc_1 inhibitor design and inform epidemiological studies of atovaquone resistance.

Atovaquone is an anti-malarial drug used in combination with proguanil (*e.g.* Malarone^{TM}) for the curative and prophylactic treatment of malaria. Atovaquone, a 2-hydroxynaphthoquinone, is a competitive inhibitor of the quinol oxidation (Q_o) site of the mitochondrial cytochrome bc_1 complex. Inhibition of this enzyme results in the collapse of the mitochondrial membrane potential, disruption of pyrimidine biosynthesis, and subsequent parasite death. Resistance to atovaquone in the field is associated with point mutations in the Q_o pocket of cytochrome *b*, most notably near the conserved Pro^{260}-Glu^{261}-Trp^{262}-Tyr^{263} (PEWY) region in the ef loop). The effect of this mutation has been extensively studied in model organisms but hitherto not in the parasite itself. Here, we have performed a molecular and biochemical characterization of an atovaquone-resistant field isolate, TM902CB. Molecular analysis of this strain reveals the presence of the Y268S mutation in cytochrome *b*. The Y268S mutation is shown to confer a 270-fold shift of the inhibitory constant (K_i) for atovaquone with a concomitant reduction in the V_{max} of the bc_1 complex of ~40% and a 3-fold increase in the observed K_m for decylubiquinol. Western blotting analyses reveal a reduced iron-sulfur protein content in Y268S bc_1 suggestive of a weakened interaction between this subunit and cytochrome *b*. Gene expression analysis of the TM902CB strain reveals higher levels of expression, compared with the 3D7 (atovaquone-sensitive) control strain in bc_1 and cytochrome *c* oxidase genes. It is hypothesized that the observed differential expression of these and other key genes offsets the fitness cost resulting from reduced bc_1 activity.

Atovaquone is a potent and effective antimalarial drug when used as a fixed dose combination with proguanil (Malarone^{TM}), either for treating children and adults with uncomplicated *Plasmodium falciparum* malaria (1, 2) or as a chemoprophylaxis for preventing malaria in travelers (3).

Atovaquone, a hydroxynapthoquinone, is a competitive inhibitor of ubiquinone, specifically inhibiting *Plasmodium* mitochondrial bc_1 activity (4). The loss of bc_1 activity results in a loss of mitochondrial function as evidenced by the collapse of the transmembrane electrochemical potential (5, 6). It is believed that in asexual parasites, one of the essential functions of the mitochondrion is to provide orotate for pyrimidine biosynthesis through the activity of dihydroorotate dehydrogenase (DHODH). Consistent with this, inhibition of the bc_1 complex by atovaquone results in an increase in carbamoyl-aspartate and a reduction in UTP, CTP, and dTTP (7, 8). A link between mitochondrial function and pyrimidine biosynthesis is further supported by the generation of an atovaquone-resistant phenotype in transgenic *P. falciparum* parasites expressing ubiquinone-independent yeast DHODH (2). Atovaquone has also recently been shown to affect the conversion of fumarate to aspartate, further linking mitochondrial function with pyrimidine biosynthesis and also possibly purine metabolism (9).

At the structural level, details of atovaquone binding to cytochrome *b* are based on studies performed on model organisms and molecular modeling because a crystal structure of the *P. falciparum* cytochrome bc_1 complex is not available. This notwithstanding, EPR spectroscopy of the Rieske [2Fe-2S] cluster, site-directed mutagenesis of model organism cytochrome *b*,

* This work was supported by grants from the Leverhulme Trust, the Wellcome Trust, the European Union Framework 7 Marie Curie Initial Training Network 215281 (InterMalTraining), the Malaysian Government, and the National Institute of Health Research (BRC Liverpool).
⌘ *Author's Choice*—Final version full access.
[S] This article contains supplemental Tables S1 and S2.
[1] These authors contributed equally to this work.
[2] Present address: Department of Microbiology and Parasitology, Faculty of Medicine and Health Sciences, Universiti Putra Malaysia, 43400 Serdang, Selangor Darul Ehsan, Malaysia.
[3] To whom correspondence may be addressed: Liverpool School of Tropical Medicine, Pembroke Place, Liverpool L3 5QA, UK. Tel.: 441517052563; Fax: 441517053371; E-mail: saward@liv.ac.uk.
[4] To whom correspondence may be addressed: Liverpool School of Tropical Medicine, Pembroke Place, Liverpool L3 5QA, UK. Tel.: 441517053151; Fax: 441517053371; E-mail: Biagini@liverpool.ac.uk.

and gene sequencing of atovaquone-resistant *Plasmodium* species demonstrate that atovaquone is most likely a competitive inhibitor of the parasite's cytochrome *b* quinone oxidation (Q_o)[5] site (reviewed in Refs. 10 and 11).

Atovaquone-resistant isolates of *P. falciparum* have been described following atovaquone or Malarone™ treatment failures. In these parasite lines, atovaquone drug failure is associated with a mis-sense point mutation at position 268 in cytochrome *b*, exchanging tyrosine for serine (Y268S) or, less frequently, asparagine (Y268N) (12–17). The resultant atovaquone-resistant growth IC_{50} phenotype of these mutants is some 1000-fold higher than sensitive strains.

Position 268 in cytochrome *b* is highly conserved across all phyla. It is located within the "ef" helix component of the Q_o site, and it is likely that the side chain of this residue participates in a stabilizing hydrophobic interaction with bound ubiquinol. Similarly, molecular modeling indicates a stabilizing interaction of Tyr^{268} in the binding of atovaquone to yeast cytochrome *b* (10). In yeast, the introduction of the Y268S mutation (Y279S) results in an increase in IC_{50} for atovaquone inhibition of bc_1 enzymatic activity from 60 nM to >4000 nM (18). However, this is accompanied by a 70% reduction in bc_1 turnover, with EPR analysis showing an alteration of the ISP signal, indicative of a perturbation of the Q_o site (18, 19).

To date there are no data available concerning the effect of the atovaquone resistance mutation on the parasite bc_1 enzyme. *Plasmodium* cytochrome *b* shares a high degree of sequence and structural conservation with mammalian and yeast cytochrome *b*; however, there are notable differences in key regions of the malaria parasite Q_o site. These include a four-residue deletion in the cd2 helix, which is based on a homology model of the *P. falciparum* cytochrome *b* (constructed using bovine cytochrome *b* atomic coordinates as the structural template (20)) and results in a 13 Å displacement of this structural element compared with the mammalian enzyme (20). Likewise, the α-carbon atom of the N-terminal proline of the ef helix (containing the catalytically essential PEWY motif) is predicted to be displaced by 2 Å compared with the mammalian enzyme. The differences in *Plasmodium* cytochrome *b* compared with yeast or mammalian cytochrome *b* are manifested by the varying degrees of susceptibility to Q_o site inhibitors, *e.g.* WR249685 is active at 3 nM against *P. falciparum* bc_1 compared with >13,800 nM for bovine bc_1 and >5600 nM for yeast bc_1 (20). The described differences between model organism bc_1 and parasite bc_1 therefore highlight the need to study this enzyme complex from parasite-derived preparations.

In this study we have investigated the effect of mutation of the conserved tyrosine 268 on the enzymatic turnover and stability of *P. falciparum* bc_1. In addition, we report the expression profile of energy metabolism genes from atovaquone-sensitive and -resistant parasites and discuss these data in the context of the structure and function of the enzyme and with regard to the possible metabolic adaptations that accommodate mutations in bc_1.

[5] The abbreviations used are: Q_o, quinol oxidation; DHODH, dihydroorotate dehydrogenase; ISP, iron-sulfur protein; Cyt, cytochrome.

EXPERIMENTAL PROCEDURES

Parasites, Culture, and Drug Sensitivity Testing—*Plasmodium falciparum* (3D7 strain) cultures consisted of a 2% (v/v) suspension of O+ erythrocytes in RPMI 1640 medium (R8758, glutamine, and $NaHCO_3$) supplemented with 10% pooled human AB+ serum, 25 mM HEPES (pH 7.4), and 20 μM gentamicin sulfate (21). The cultures were grown under a gaseous headspace of (in v/v) 4% O_2, 3% CO_2 in N_2 at 37 °C. Parasite growth was synchronized by treatment with sorbitol (22).

Drug susceptibilities were assessed by the measurement of fluorescence after the addition of SYBR Green I as described in Ref. 23. Drug IC_{50} values were calculated from the log of the dose/response relationship, as fitted with Grafit software (Erithacus Software, Kent, UK). The results are given as the means of at least three separate experiments.

The atovaquone-resistant TM90C2B was generously provided by Prof. Dennis Kyle (College of Public Health, University of South Florida, Tampa, FL) and was first isolated during a clinical phase 2 study to determine atovaquone efficacy in Thailand (24).

Transgenic Parasites—3D7-yDHODH·GFP, a transgenic derivative of *P. falciparum* 3D7 containing yeast dihydroorotate dihydrogenase, was generated through electroporation of purified pHHyDHOD-GFP plasmid into ring stages of *P. falciparum* using a Bio-Rad GenePulser following the method of Painter *et al.* (2). Purified pHHyDHOD-GFP plasmid was generously provided by Prof. Akhil Vaidya (Drexel University College of Medicine, Philadelphia, PA). This plasmid contains a human dihydrofolate reductase gene as a WR99210-selectable marker (2).

Preparation of P. falciparum Cell-free Extracts—Free parasites were prepared from aliquots of infected erythrocytes (~8×10^9 cells ml^{-1}) by adding 5 volumes of 0.15% (w/v) saponin in phosphate-buffered saline (137 mM NaCl, 2.7 mM KCl, 1.76 mM K_2HPO_4, 8.0 mM Na_2HPO_4, 5.5 mM D-glucose, pH 7.4) for 5 min, followed by three washes by centrifugation and resuspension in HEPES (25 mM)-buffered RPMI containing a protease inhibitor mixture (Complete Mini; Roche Applied Science). Cell extract was prepared by repeated freeze-thawing in liquid N_2, followed by disruption with a sonicating probe.

Preparation of Bovine Crude Mitochondrial Membranes—Bovine mitochondrial membranes (Keilin-Hartree particles) were prepared as described by Kuboyama *et al.* (25).

Preparation of Decylubiquinol—The artificial quinol electron donor was prepared based on our previously described method (26). Briefly, 2,3-dimethoxy-5-methyl-*n*-decyl-1,4-benzoquinone (decylubiquinone), an analog of ubiquinone (Sigma), was dissolved (10 mg) in 400 μl of nitrogen-saturated hexane. An equal volume of aqueous 1.15 M sodium dithionite was added, and the mixture was shaken vigorously until colorless. The upper, organic phase was collected, and the decylubiquinol recovered by evaporating off the hexane under N_2. The decylubiquinol was dissolved in 100 μl of 96% ethanol (acidified with 10 mM HCl) and stored in aliquots at −80 °C. Decylubiquinol concentration was determined spectrophotometrically from absolute spectra, using $\epsilon_{288-320} = 4.14\ mM^{-1}\ cm^{-1}$.

Measurement of Decylubiquinol:Cytochrome c Oxidoreductase Activity—Cytochrome *c* reductase activity measurements were assayed in a Cary 4000 spectrophotometer at 500 *versus* 542 nm in a reaction buffer consisting of 50 mM potassium phosphate (pH 7.5), 2 mM EDTA, 10 mM KCN, and 30 μM equine cytochrome *c* (Sigma) at room temperature (26). The reaction volume was 700 μl. *P. falciparum* bc_1 was present as a crude membrane preparation ("cell-free extract") at a total protein concentration of 30–60 μg/ml. Cytochrome *c* reductase activity was initiated by the addition of decylubiquinol (5–50 μM), and the kinetic data were collected for 4 min. Initial rates (computer-fitted as zero order kinetics) were measured as a function of decylubiquinol concentration, using $\epsilon_{550-542} = 18.1\ \text{mM}^{-1}\ \text{cm}^{-1}$.

Sequencing Cytochrome b of P. falciparum TM90C2B—The sequences of the primers used for PCR amplification of the genes encoding cytochrome *b* and the ISP from TM90C2B cDNA were as follows: Cyt b forward, 5′-ATGAACTTTTACTCTATTAATTTAG; Cyt b reverse, 5′-TATGTTTGCTTGGGAGCTGTAATC; ISP forward, 5′-ATGAATATTAAATATGTGGAAC; and ISP reverse, 5′-TCCAATTTTTATCGTATTTTCAT. The PCR consisted of 96 °C for 10 min followed by 25 reaction cycles with melting (45 s), annealing (45 s), and extension (2 min) temperatures of 96, 45, and 68 °C, respectively, with a final 10-min extension at 68 °C. The PCR buffer contained 1 mM $MgSO_4$, 100 ng of TM90 cDNA, 0.25 mM dA/C/G/TTP (1 mM total dNTP), 1× *Pfx* proprietary reaction buffer (Invitrogen), 2 μM forward/reverse primers, and 1 unit of *Pfx* DNA polymerase (Invitrogen). Total reaction volume was 50 μl. The PCR products were purified by 2% (w/v) agarose gel electrophoresis and sent for automated DNA sequencing (Lark Technologies, Takeley, UK). Sequence chromatograms were inspected using the 4Peaks software package.

Expression Profile of Energy Metabolism Genes from Wild Type, Transgenic, and Atovaquone-resistant P. falciparum Parasites—Quantitative RT-PCR was used to determine the expression of energy metabolism genes from 3D7, 3D7-yDHODH·GFP, and TM90C2B parasites. RNA was extracted from highly synchronized (>99%) trophozoite stage parasites on at least three independent occasions. Aliquots (75 ng) from each pool of total RNA served as templates for making target specific cDNA by reverse transcription in a single multiplex assay using the GenomeLab GeXP Start Kit (Beckman Coulter) and the gene-specific primers in supplemental Table S1. The primers were designed using the eXpres Profiler software (Beckman Coulter) based on cDNA sequences retrieved from Plasmo.DB. The GeXP multiplex system uses a combined target-specific primer and a universal sequence to reverse transcribe mRNA into cDNA. The reverse transcription step was followed by a PCR step in which during the first three cycles of amplification were carried out by chimerical forward and reverse primers (supplemental Table S1). For subsequent cycles (cycles 4–35), amplification was carried out using universal forward and universal reverse primers provided by the kit. The PCR conditions were 95 °C for 10 min, followed by 35 cycles of 94 °C for 30 s, 55 °C for 30 s, and 68 °C for 1 min. Multiplexing primer specificity was confirmed by sequencing the PCR products obtained from single reactions. The universal primers that come with the kit were fluorescently labeled and yielded signals that corresponded to the amount of product in the multiplex reaction. PCR products were quantified with a CEQ 8000 Genetic Analysis System (Beckman Coulter) running a GenomeLab GeXP eXpress analysis program (Beckman Coulter) that computes peak areas for each target. The peak area of a reference gene, elongation factor 1α (PlasmoDB accession PF13_0305) was used to normalize for variation in the total mRNA amount. Normalized peak areas were then log2-transformed to approximate a normal distribution. To determine whether there was any interference from sexual stage-dependent gene expression, sexual development was measured by analysis of Pfs16 gene expression (PlasmoDB accession PF11_0318) (27).

Anti-bc_1 Polyclonal Antibody Synthesis—The peptide ^{322}SHYDNSGRIRQGPA^{335} of the ubiquinol-cytochrome *c* reductase Rieske iron-sulfur subunit (Swissprot accession number Q8IL75) of the *Plasmodium falciparum* bc_1 protein was selected, synthesized, and used for immunization in the rabbit and generation of an affinity-purified polyclonal antibody (GenScript Corp., Piscataway, NJ). The rabbit anti-Pfbc1 polyclonal antibodies were lyophilized in phosphate-buffered saline (pH 7.4) with 0.02% sodium azide as preservative. Lyophilized antibodies were reconstituted with MilliQ water, and aliquots were stored at −20 °C until use.

Free Parasites Membrane Protein Extraction—Free parasites were harvested at the trophozoite stage with a parasitemia >8% by treatment with 0.15% (w/v) saponin in phosphate-buffered saline. After three washes in 25 mM HEPES-buffered RPMI 1640 by centrifugation at 4 °C at 6,000 × *g* for 5 min, the cells were disrupted with a sonicating probe in lysis buffer (50 mM Tris-HCl, 150 mM NaCl, 2 mM EDTA, pH 7.4) in the presence of protease inhibitor mixture (Complete Mini; Roche Applied Science). Lysate was centrifuged at 17,000 × *g* for 30 min at 4 °C, and the membrane proteins of the parasites (pellet) were separated from the soluble proteins (supernatant).

Immunoprecipitation—For immunoprecipitation studies, membrane proteins were boiled (5 min at 95 °C) in denaturing lysis buffer (50 mM Tris-HCl, 5 mM EDTA, 2% (w/v) SDS, 10 mM DTT) and diluted (10-fold) with nondenaturing lysis buffer (50 mM Tris-HCl, 150 mM NaCl, 1 mM EDTA, 1% (v/v) Triton X-100, pH 7.5). Following centrifugation (17,000 × *g* for 30 min), denatured proteins were collected in the supernatant and incubated overnight with 2 μg of anti-*bc1* antibody, rotating at 4 °C, followed by 50 μl of protein A-Sepharose slurry for 3 h at 4 °C. Immunoprecipitates were washed, gently eluated with an acidic buffer (pH 2.8), and then separated by 10% (w/v) SDS-PAGE gel electrophoresis before proceeding to immunoblotting.

Immunoblotting—Antigens obtained were separated by 10% (w/v) SDS-PAGE gel electrophoresis and transferred to Hybond ECL nitrocellulose (GE Healthcare). The membranes were saturated overnight at 4 °C in blocking solution (5% (w/v) dry milk powder, 0.05% (v/v) Tween 20 in PBS solution), and the immunodetection was carried out 2 h with the anti-bc_1 antibody polyclonal antibody. A second incubation of 1 h with a rabbit primary polyclonal antibody against *P. falciparum* aldolase was performed as a loading control (28). Horseradish per-

oxidase-conjugated goat anti-rabbit IgG secondary antibody was used at 1:10000 dilution for 1 h. The signal was visualized by chemiluminescence with ECL™ Western blotting detection reagent kit (Amersham Biosciences), followed by exposure of the membranes to Kodak® BioMax™ MR film.

In-gel Trypsin Digestion, Mass Spectrometry, and Database Searches—An identical SDS-PAGE was silver-stained, and protein spots corresponding to the signal from the anti-bc_1 immunoblot were excised. Each sample was reduced with 10 mM DTT at 56 °C for 30 min and alkylated with 55 mM iodoacetamide at 37 °C for 30 min. Proteins contained within these gel spots were proteolyzed by addition of 190 ng of sequencing grade trypsin (Sigma) and incubated overnight at 37 °C. The resulting tryptic peptides were then dried and rehydrated in 5% (v/v) formic acid in 50% (v/v) acetonitrile. NanoLC-MS/MS analyses were performed on a Dual Gradient Ultimate 3000 chromatographic system (Dionex). A 20-μl aliquot of sample was placed into a well on a 96-well plate, of which 10 μl of sample was injected onto a C18 precolumn (Acclaim PepMap C18; 2-cm length × 100-μm inner diameter × 5-μm particle size; 100 Å porosity; Dionex). After desalting for 6 min with buffer A (water/acetonitrile/formic acid, 97.5/2.5/0.1 v/v/v) peptide separation was carried out on a C18 capillary column (Acclaim PepMap C18; 15-cm length × 75-μm inner diameter × 2-μm particle size; 100 Å porosity; Dionex) with a gradient method starting at 100% buffer A, ramping up to 50% buffer B (water/acetonitrile/formic acid, 10/90/0.1 v/v/v) over 90 min. This was then increased to 100% buffer B over 0.1 min, which was then held at 100% buffer B for 10 min. Finally, this was decreased to 0% over 0.1 min, and buffer A was increased to 100%. The column was finally re-equilibrated with 100% buffer A for 15 min. The LC eluent was nano-sprayed into the MS instrument with a glass emitter tip (Pico-tip, FS360 –50-15-CE-20-C10.5; New Objective Woburn). The LTQ-Orbitrap Velos mass spectrometer (ThermoFisher Scientific) was operated in positive ionization mode. Raw data files were processed using the software Proteome Discoverer 1.0.0 (ThermoScientific) incorporating Sequest search algorithm. The proteins were identified by screening LC-MS sequence data against a PlasmoDB database (version 8.0). A parent mass tolerance of 1.5 Da and fragment mass tolerance of 1 Da were used, allowing for one missed cleavage. Carbamidomethylation of cysteine and oxidation of methionine were the fixed and variable modifications, respectively.

Molecular Modeling of the Yeast (Saccharomyces cerevisiae) bc_1 *Q_o Site Atovaquone Interaction*—GOLD 5.0.1 (CCDC Software Limited, Cambridge, UK) was used to dock atovaquone into the Q_o site of the yeast cytochrome bc_1 complex (Protein Data Bank code 3CX5) (29). The hydroxyl moiety of atovaquone was modeled in the protonated form. The native ligand stigmatellin was removed and used to define the binding site as 6 Å around the ligand. Protons were added, and all of the crystallographic water molecules were removed, except HOH7187, which has previously been described as key to the observed hydrogen bonding network (31). Constraints were applied such that docking poses were optimized to form the His^{181} and Glu^{272} interactions, with HOH7187 allowed to spin and translate from its original position within a radius of 2 Å. Docking was performed using the GoldScore scoring function, with the reported pose having a GoldScore of 29.02.

RESULTS

Sequencing of Cytochrome b in TM90C2B—Automated DNA sequencing of the mitochondrial cytochrome *b* gene PCR-amplified from *P. falciparum* TM90C2B cDNA confirmed the mutation of adenine to cytosine at nucleotide 803, resulting in the replacement of tyrosine by serine at amino acid position 268 (data not shown). No additional mutations were observed in the nucleotide sequence of TM90C2B cytochrome *b* or the Rieske (ISP) protein when compared with the control DNA (*P. falciparum* 3D7; data not shown).

Inhibition Profile of Atovaquone-sensitive and -resistant Strains—Growth inhibition assays were performed to confirm the phenotypic profiles of the wild type (3D7) and atovaquone-resistant strains (TM90C2B and 3D7-yDHODH·GFP) to therapeutic drugs and various specific electron transport inhibitors. As expected, 3D7-yDHODH·GFP was highly resistant to atovaquone and other bc_1-targeting inhibitors (antimycin and stigmatellin), consistent with the original work performed by Painter *et al.*, (2). Also as expected, TM90C2B harboring the Y268S mutation in bc_1 was shown to be highly resistant (>12,000-fold) to atovaquone. Interestingly however, TM902CB also displayed an increased resistance to other bc_1 inhibitors including the Q_o site inhibitors myxothiazol (~20-fold) and stigmatellin (~5-fold), as well as the Q_i site inhibitor antimycin (~20-fold). A ~20-fold increase in the IC_{50} of the Complex II inhibitor 2-thenoyltrifluoroacetone against TM902CB relative to 3D7 was also observed, whereas Complex IV inhibition by azide and DHODH inhibition by 5-fluoroorotic acid were similar between 3D7 and TM902CB (Table 1).

Loss of Conserved Tyrosine Reduces Catalytic Activity of P. falciparum bc_1—We next determined what effect the Y268S mutation would have on the enzymatic activity of the parasite bc_1 complex. Steady-state kinetics parameters were determined for wild type (3D7) and atovaquone-resistant (TM90C2B) *P. falciparum* bc_1. The dQH2:Cyt *c* oxidoreductase V_{max} was measured as 97.4 ± 5.1 and 60.2 ± 3.2 nmol of Cyt *c* reduced/min/mg of protein for 3D7 and TM90C2B, respectively (Fig. 1*a* and Table 2), although the K_m for dQH2 was determined to be 5.5 ± 1.1 and 18.5 ± 2.6 μM for 3D7 and TM90C2B, respectively (Fig. 1*a* and Table 2).

In our standard assay conditions, dQH2:Cyt *c* oxidoreductase activity from wild type (3D7) parasite was inhibited by atovaquone with an IC_{50} of 6 ± 1 nM, whereas TM90C2B parasite dQH2:Cyt *c* oxidoreductase activity was inhibited with an IC_{50} of 600 ± 90 nM (Fig. 1*b*). The inhibition constant (K_i) for atovaquone for 3D7 and TM90C2B was 0.6 and 162 nM, respectively (calculated from the Cheng-Prusoff equation (30), assuming competitive inhibition with dQH2).

Characterization of the Anti-bc_1 Antibody—To measure bc_1 protein expression in the parasite, a custom polyclonal antibody against the Rieske subunit of the *P. falciparum* bc_1 complex was raised using a commercial supplier (GenScript Corp.). To validate this customized antibody by analysis of its antigens with NanoLC-MS/MS, an immunoprecipitation experiment

TABLE 1

Growth inhibition profiles of P. falciparum 3D7, 3D7-yDHODH·GFP, and TM90C2B parasites

The data are expressed as the means ± S.E., acquired from multiple replicates performed on at least three independent occasions. The IC_{50} values were calculated by fitting of four-parameter logistic curves (Grafit software). ND, not determined.

Drug	Target	IC_{50}		
		3D7	3D7-yDHODH·GFP	TM90C2B
			nM	
Artesunate		1.6 ± 0.4	1.1 ± 0.1	0.5 ± 0.1
Chloroquine		11.4 ± 0.4	10.4 ± 0.4	70.6 ± 9.6
Atovaquone	bc_1 (Q_o)	0.8 ± 0.1	$5.8 \times 10^3 \pm 2.2 \times 10^3$	$12.4 \times 10^3 \pm 1.6 \times 10^3$
Stigmatellin	bc_1 (Q_o)	23.2 ± 4.2	$4.1 \times 10^3 \pm 425$	107 ± 13
Myxothiazol	bc_1 (Q_o)	33.3 ± 6.4	ND	564 ± 11
Antimycin	bc_1 (Q_i)	13.8 ± 2.2	ND	300 ± 34
2-Thenoyltrifluoroacetone	Succinate dehydrogenase	$1.5 \times 10^3 \pm 245$	$1.4 \times 10^3 \pm 352$	$31.4 \times 10^3 \pm 965$
Sodium azide	Cyt aa_3	$423 \times 10^3 \pm 45 \times 10^3$	$586 \times 10^3 \pm 97 \times 10^3$	$654 \times 10^3 \pm 102 \times 10^3$
5-Fluoro-orotic acid	Dihydroorotate dehydrogenase	6.1 ± 0.9	5.5 ± 0.4	6.3 ± 1.3
Pyrimethamine	Dihydrofolate reductase	31.5 ± 6.9	$35.9 \times 10^3 \pm 9.9 \times 10^3$	>10,000

was performed on the membrane proteins obtained from 3D7 free-parasite extracts. The result of the immunocapture (separated by 10% SDS-PAGE) was observed by Western blot and silver staining (Fig. 2). The immunoblot revealed a protein captured around 41 kDa, consistent with the size of the Rieske subunit in the malaria parasite. The band corresponding to the protein was excised from the silver-stained gel, digested with trypsin, and analyzed by NanoLC-MS/MS to obtain the peptide sequence data. The Rieske subunit was identified by 28 peptide mass fingerprints with sequence coverage of 60.0%. An example of the NanoLC-MS/MS fragmentation pattern of the peptide ^{101}YAHYNQTAEPVPR^{114} is shown in Fig. 3. Attempts to generate polyclonal antibodies specific to *P. falciparum* cytochrome *b* were unsuccessful.

Cytochrome b Protein Expression in Atovaquone-sensitive and -resistant Parasites—Using the characterized anti-ISP antibody, the extent to which the Y268S mutation affected protein expression was determined by performing Western blots of cell-free extracts prepared from TM90C2B compared with the atovaquone-sensitive 3D7 strain. As shown in Fig. 4 (*top panel*), a decrease in ISP content was observed in Western blots prepared from TM90C2B compared with the 3D7 control strain. This experiment was performed on three separate occasions using different membrane preparations. For all experiments, aldolase was used to control for any potential differences in protein loading (Fig. 4). In contrast to the parasite data, no such loss in the ISP signal was observed using crude mitochondrial membranes prepared from yeast containing the Y279S cytochrome *b* mutation, relative to wild type control (data not shown).

Transcriptional Expression Profiles of Energy Metabolism Genes in Atovaquone-sensitive and -resistant Parasites—To determine whether any of the phenotypic differences between TM90C2B and 3D7 could be accounted for by differential gene expression, quantitative RT-PCR was used to determine the expression of energy metabolism genes from 3D7 and TM90C2B parasites. Gene expression from the transgenic strain 3D7-yDHODH·GFP, harboring the yeast DHODH, which confers an atovaquone-resistant phenotype (2), was also determined because this strain should show a similar expression profile to its parent 3D7 strain. The 36 genes that were monitored included those involved in glycolysis/fermentation, specific subunits of mitochondrial electron transport chain complexes, mitochondrial dehydrogenases, and mitochondrial Krebs cycle genes. Expression profiles from the various strains were measured from RNA taken from trophozoite-stage parasites on at least three independent occasions; expression was then normalized against the expression of a reference gene, elongation factor 1α (see methods). Mean expression levels ($n \geq 3$) for all of the genes from the three strains are given in supplemental Table S2. Fig. 5 shows the relative fold change in gene expression for (*a*) 3D7-yDHODH·GFP/3D7 and (*b*) TM90C2B/3D7. As expected, the transgenic 3D7-yDHODH·GFP strain displayed relatively little difference in the fold change in gene expression compared with 3D7 and with the exception of one gene (NAD glutamate dehydrogenase); all of the expression values fell at or near 1 (Fig. 5*a*).

However, analysis of the fold change in gene expression of the atovaquone-resistant strain TM90C2B compared with the atovaquone-sensitive 3D7 strain revealed some significant differences between the two strains (Fig. 5*b*). Of note was the ~2-fold increase in expression of Complex III and Complex IV genes, which included cytochromes *b*, *c*, and c_1; the Rieske (ISP) subunit of bc_1; and subunits 1 and 2 of cytochrome *c* oxidase (Fig. 5*b* and supplemental Table S2). Other genes also shown to have higher comparative levels of expression (by up to 2-fold) included the hexose transporter, phosphoglycerate kinase and succinyl CoA synthetase.

Both TM90C2B and 3D7 are able to generate gametocytes in the laboratory. Analysis of the sexual development gene pfs16 revealed no change in expression levels during replication or between strains (supplemental Table S2 and Fig. 5), indicating that measured gene expression from these strains was not a consequence of sexual development.

DISCUSSION

In the absence of a crystal structure for *P. falciparum* bc_1, an *in silico* model of atovaquone docked at the Q_o site of yeast cytochrome *b* has been described by Kessl *et al.* (31) that performs as a useful surrogate for discussion. We present an updated version of the atovaquone-bound yeast model in Fig. 6. In the yeast model, atovaquone is represented as a "heme-distal" Q_o inhibitor, binding in a manner strongly reminiscent of stigmatellin. In the model, the hydroxyl moiety of the hydroxynaphthoquinone ring of atovaquone forms a hydrogen bond to the ϵN atom of the imidazole group of His^{181} in the

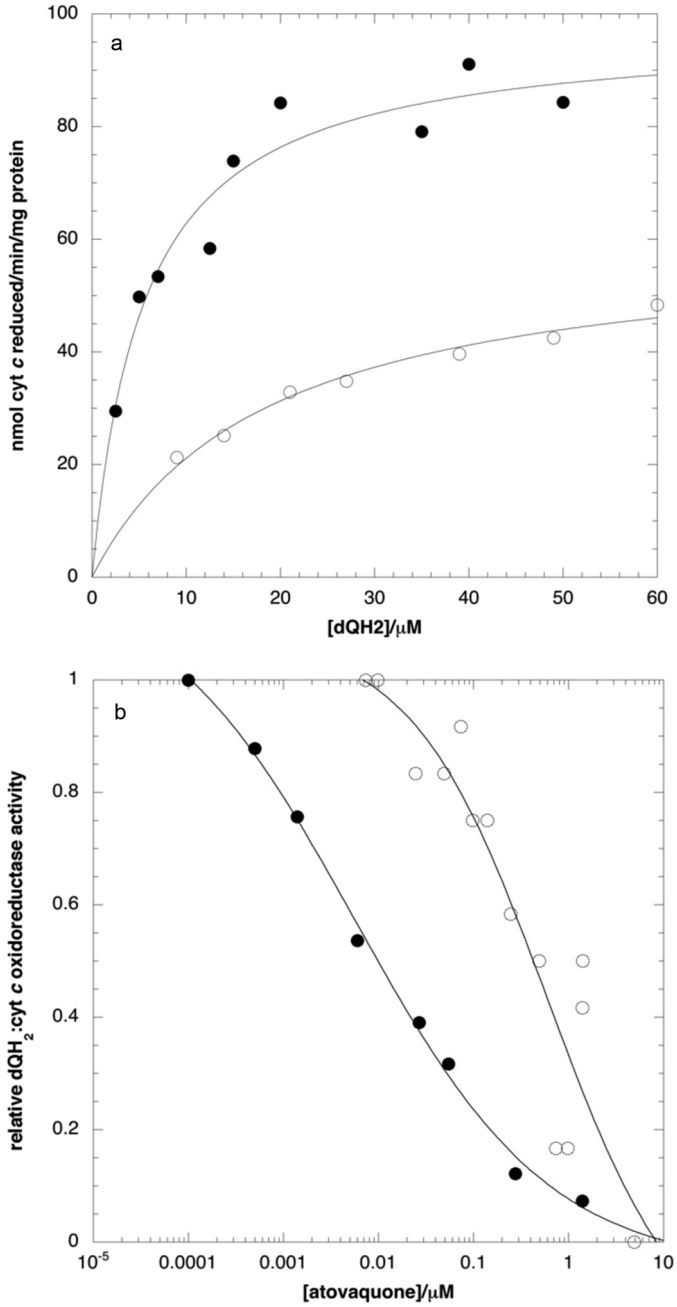

FIGURE 1. *a*, steady-state decylubiquinol:cytochrome *c* oxidoreductase activity of *P. falciparum* 3D7 (●) and TM90C2B (○) bc_1 in crude cell-free extracts. The assays were performed as described under "Experimental Procedures" and consist of the combined kinetic data from three separate experiments per strain. The data were fitted to a Michaelis-Menten rectangular hyperbola using Kaleidagraph (Synergy Software). *b*, inhibition of steady-state decylubiquinol:cytochrome *c* oxidoreductase activity of *P. falciparum* 3D7 (●) and TM90C2B (○) bc_1 in crude cell-free extracts by atovaquone. The assays were performed as described under "Experimental Procedures" using a decylubiquinol concentration of 50 μM. The data were fitted using a four-parameter sigmoidal function in Kaleidagraph (Synergy Software).

Rieske iron-sulfur protein (lowering the redox potential of the [2Fe-2S] cluster). A second H-bond is formed between the hydroxynaphthoquinone carbonyl group of atovaquone and the carboxylate of cytochrome *b* ef loop residue Glu^{272} via a bridging water molecule. The chlorophenyl ring of atovaquone in the yeast model sits in a hydrophobic pocket within cytochrome *b* formed from the side chains of Phe^{121} (transmembrane helix C) and Phe^{278} (ef loop). Leu^{275} (ef loop) is predicted to form a stabilizing hydrophobic contact with the cyclohexyl moiety of atovaquone. A similar pocket is likely to be formed by the corresponding residues in *P. falciparum* cytochrome *b* (Phe^{115}, Phe^{264}, and Phe^{267}).

Tyr^{268} (*Plasmodium* notation), located within the ef helix, is highly conserved. In yeast, it has been suggested that the tyrosyl side chain of this residue participates in the positioning of Q_o-bound ubiquinol, and it has been postulated to contribute to stabilizing hydrophobic interactions with the naphthoquinone group of atovaquone (31, 32). Studies with mutant forms of bc_1 from the bacterium *Rhodobacter sphaeroides* indicated that an aromatic or large hydrophobic side chain residue is required at this position within the ef helix for efficient catalytic activity (33). A recent examination of the crystal structure of avian bc_1 suggests a role for the hydroxyl moiety of this side chain in the formation of a hydrogen-bonding association with His^{181} of the Rieske protein (34). In addition, mutation of the equivalent residue in man (Tyr-279) has been linked with a variety of mitochondrial disorders (26, 35). To date, there are no atomic structures available for bc_1 complex with Q_o-bound ubiquinol.

The decrease in V_{max} reported here in crude preparations of TM90C2B bc_1 (60.2 ± 3.2 nmol Cyt *c* reduced/min/mg protein) compared with the control 3D7 strain (97.4 ± 5.1 nmol of Cyt *c* reduced/min/mg of protein) is similar to that observed for the yeast Y279C and Y279S mutants (turnover numbers of 47 and 30 s^{-1}, respectively, compared with the wild type value of 80 s^{-1}) (18, 26, 35), although it should be noted that more deleterious effects on the yeast enzyme activity have been noted in Y279S preparations in other laboratories (31). The 20-fold

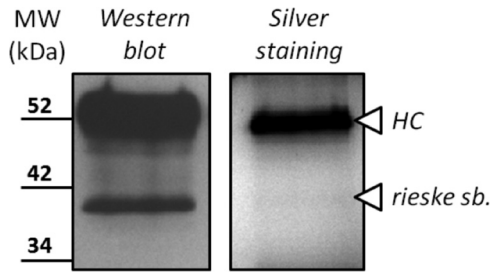

FIGURE 2. **Western blot and silver staining of the Rieske subunit (41 kDa) immunocapture from 3D7 free parasites.** HC indicate the heavy chain (50 kDa) of the polyclonal antibody used for the immunoprecipitation. *MW*, molecular mass.

TABLE 2

Cell-free extract steady-state decylubiquinol:cytochrome *c* oxidoreductase activity and atovaquone sensitivity in P. falciparum strains 3D7 and TM90C2B

Enzyme activity was measured as described under "Experimental Procedures." The K_i values for atovaquone inhibition were calculated using the Cheng-Prusoff equation (30).

P. falciparum strain	V_{max}	K_m (dQH2)	IC_{50} (atovaquone)	K_i (atovaquone)
	nmol cyt c reduced/min/mg protein	*nM*	*nM*	*nM*
3D7	97.4 ± 5.1	5.5 ± 1.1	6.4 ± 1.2	0.6
TM90C2B	60.2 ± 3.2	18.5 ± 2.6	600 ± 90	162

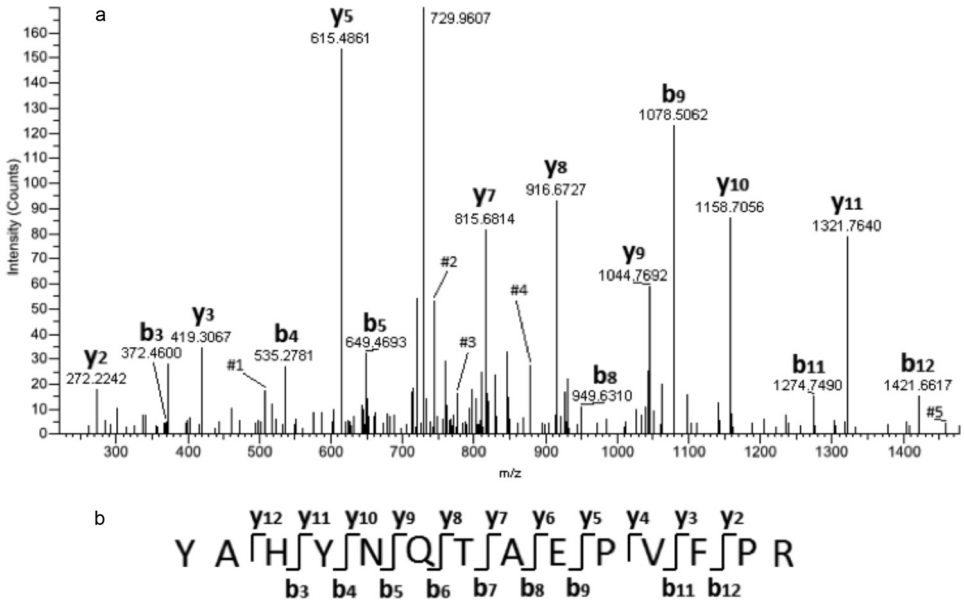

FIGURE 3. *a*, fragmentation spectra of the precursor ion with $m/z = 846.90$ Da (charge of +2) identified as peptide YAHYNQTAEPVPR (residues 101–114 of Rieske subunit). *#1*, y4 (517.3738); *#2*, y6 (744.0631); *#3*, b6 (777.4517); *#4*, b7 (878.6395); *#5*, y12 (1459.2450). *b*, peptide sequence consensus obtained after matching of y- and b-fragment ions.

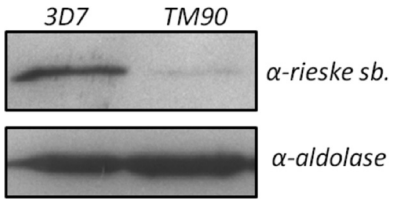

FIGURE 4. **Immunoblot analysis of the 3D7 and TM90 membrane proteins fractions with the customized anti-Rieske antibody.** Aldolase is used as a loading control and detected from their respective soluble proteins fractions.

increase in IC_{50} for the Q_i site inhibitor antimycin in TM90C2B compared with the control 3D7 strain is at first sight surprising, because the Q_o and Q_i sites are located on opposite sides of the inner mitochondrial membrane within cytochrome *b*, separated by ~25 Å. However, regulatory interactions between the Q_o and Q_i sites have been observed in yeast bc_1 in which the binding of stigmatellin affected the interaction of antimycin in a complex manner, with one half of the (dimeric) enzyme binding antimycin in a slow, concentration-independent way. Antimycin was observed to bind rapidly and in a concentration-dependent manner in the presence of myxothiazol (a "b-proximal" Q_o site inhibitor) (36). The structural mechanism for this apparent communication pathway between the quinone-binding sites within cytochrome *b* remains to be determined.

The 3-fold increase in K_m observed for decylubiquinol in TM90C2B bc_1 coupled with the decrease in V_{max} suggests that the binding and/or positioning of the substrate ubiquinol within the Q_o site is impaired in TM90C2B compared with the wild type, consistent with mutation studies of this residue in other organisms. We note with interest the apparent instability of the ISP in TM90C2B as revealed by Western blotting (Fig. 4), which suggests a weakened interaction between this subunit and cytochrome *b.* The ISP content in the corresponding yeast mutant (Y279S), however, was indistinguishable from wild type (data not shown). Similarly, in previous studies, no loss of ISP content is observed in the yeast Y279A and Y279C mutants, although the Y279W mutation was found to be structurally destabilizing (26, 31). These data further highlight the differences between parasite and yeast cytochrome *b* and the need for performing biochemical analyses on parasite material irrespective of the technical difficulties.

The instability of the ISP in TM90C2B may be due to perturbation of the ef helix and surrounding protein structure at the Q_o site caused by the introduced serinyl side chain. A potential consequence of structural perturbation around the Q_o site would be a perturbation of the docking or positioning of the ISP ecto-domain at Q_o, weakening the hydrogen bonding association and/or an increase in the electron transfer distance between bound ubiquinol and the ISP [2Fe-2S] cluster, or lowering the occupancy of bound ubiquinol. Such perturbations have been observed in Q_o site mutants of the yeast bc_1 complex (26, 37, 38). The differences in bc_1 complex integrity observed in TM90C2B and the yeast Y279S mutant may arise from the potentially unusual structure of the Q_o site and ISP docking surface in Apicomplexa (*i.e.* the four residue deletion in the N-terminal region of the cd2 helix (20)). This potential structural perturbation affecting electron transfer may also account for the apparent increased tolerance (~20-fold) that the TM902CB parasite has for heme-proximal Q_o inhibitors (*e.g.* myxothiazol), as well as Q_i inhibitors (*e.g.* antimycin; Table 1). It will be important to further understand this phenomenon because the TM902CB strain is widely used to assess the suitability of novel bc_1 inhibitors (39), and an apparent cross-resistance of novel chemotypes may be mistakenly interpreted as deriving from atovaquone-like binding.

A recent and noteworthy study by Hughes *et al.* (40) investigated the susceptibility of blood stage atovaquone-resistant (TM90C2B) and -sensitive (D6, W2) strains of *P. falciparum* to a series of novel hydroxy-naphthoquinones. The sensitivity of liver stage *Plasmodium berghei* and mutant forms of the yeast bc_1 complex to these compounds was also examined in this

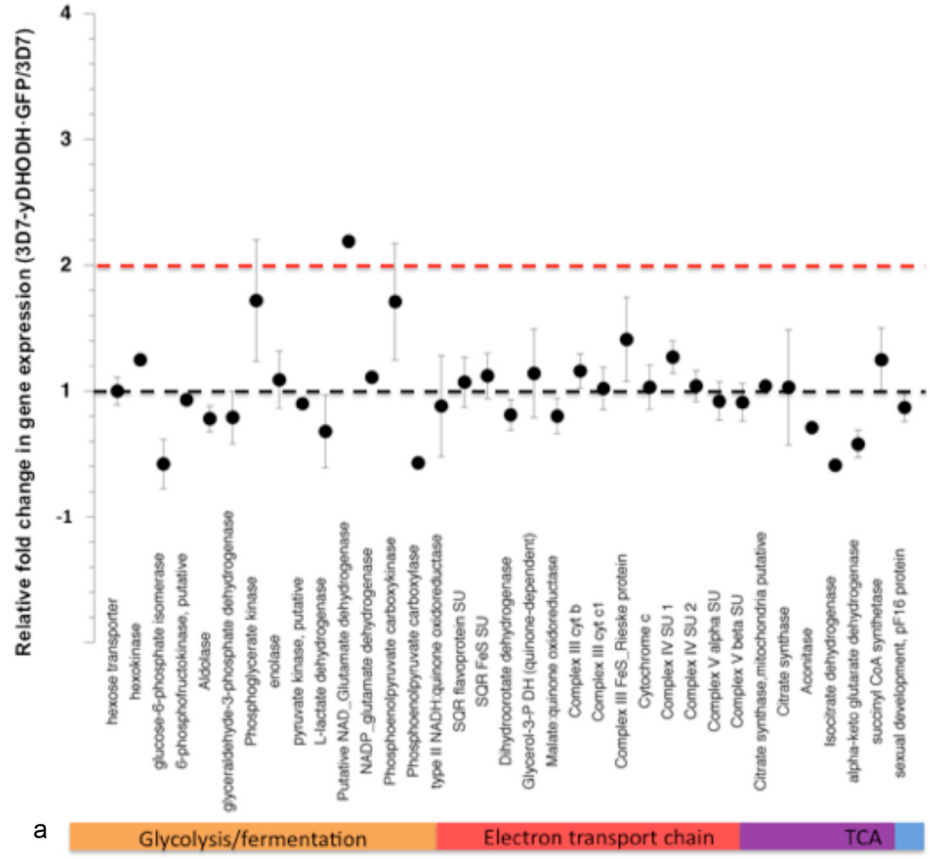
Relative fold change in gene expression (3D7-yDHODH-GFP/3D7)
4
3
2
1
-1
hexose transporter
hexokinase
glucose-6-phosphate isomerase
6-phosphofructokinase, putative
Aldolase
glyceraldehyde-3-phosphate dehydrogenase
Phosphoglycerate kinase
enolase
pyruvate kinase, putative
L-lactate dehydrogenase
Putative NAD_Glutamate dehydrogenase
NADP_glutamate dehydrogenase
Phosphoenolpyruvate carboxykinase
Phosphoenolpyruvate carboxylase
type II NADH:quinone oxidoreductase
SQR flavoprotein SU
SQR FeS SU
Dihydroorotate dehydrogenase
Glycerol-3-P DH (quinone-dependent)
Malate quinone oxidoreductase
Complex III cyt b
Complex III cyt c1
Complex III FeS_Rieske protein
Cytochrome c
Complex IV SU 1
Complex IV SU 2
Complex V alpha SU
Complex V beta SU
Citrate synthase,mitochondria putative
Citrate synthase
Aconitase
Isocitrate dehydrogenase
alpha-keto glutarate dehydrogenase
succinyl CoA synthetase
sexual development, pF16 protein
a
Glycolysis/fermentation
Electron transport chain
TCA

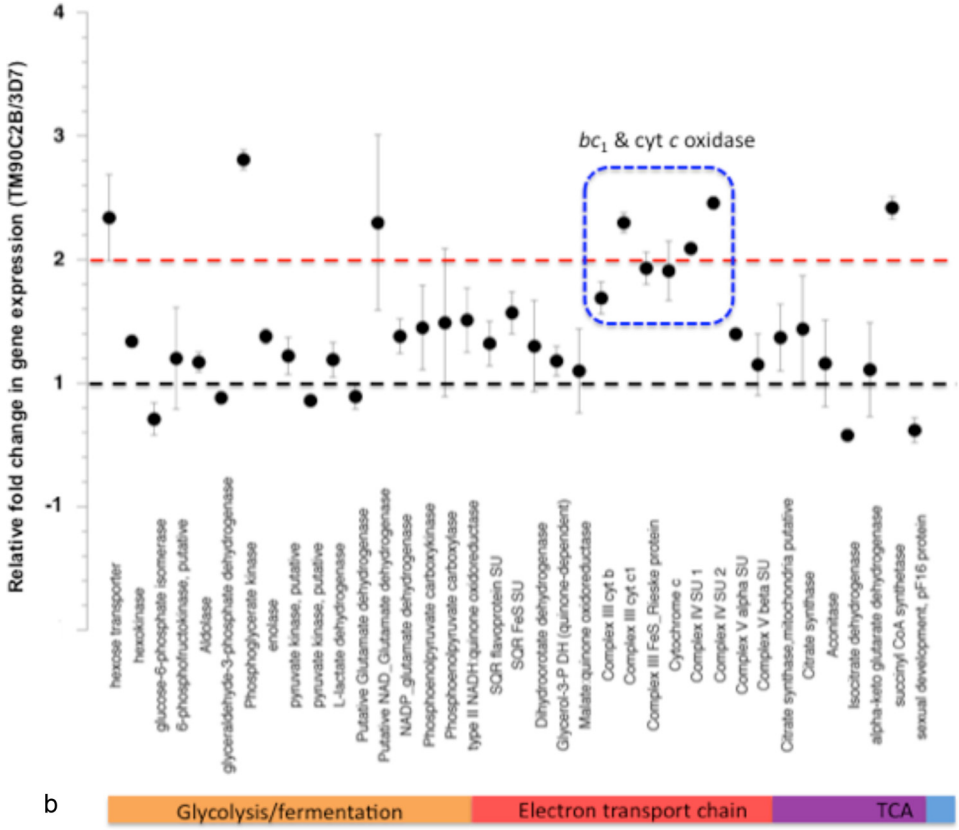
Relative fold change in gene expression (TM90C2B/3D7)
4
3
2
1
-1
bc_1 & cyt c oxidase
hexose transporter
hexokinase
glucose-6-phosphate isomerase
6-phosphofructokinase, putative
Aldolase
glyceraldehyde-3-phosphate dehydrogenase
Phosphoglycerate kinase
enolase
pyruvate kinase, putative
pyruvate kinase, putative
L-lactate dehydrogenase
Putative Glutamate dehydrogenase
Putative NAD_Glutamate dehydrogenase
NADP_glutamate dehydrogenase
Phosphoenolpyruvate carboxykinase
Phosphoenolpyruvate carboxylase
type II NADH:quinone oxidoreductase
SQR flavoprotein SU
SQR FeS SU
Dihydroorotate dehydrogenase
Glycerol-3-P DH (quinone-dependent)
Malate quinone oxidoreductase
Complex III cyt b
Complex III cyt c1
Complex III FeS_Rieske protein
Cytochrome c
Complex IV SU 1
Complex IV SU 2
Complex V alpha SU
Complex V beta SU
Citrate synthase,mitochondria putative
Citrate synthase
Aconitase
Isocitrate dehydrogenase
alpha-keto glutarate dehydrogenase
succinyl CoA synthetase
sexual development, pF16 protein
b
Glycolysis/fermentation
Electron transport chain
TCA

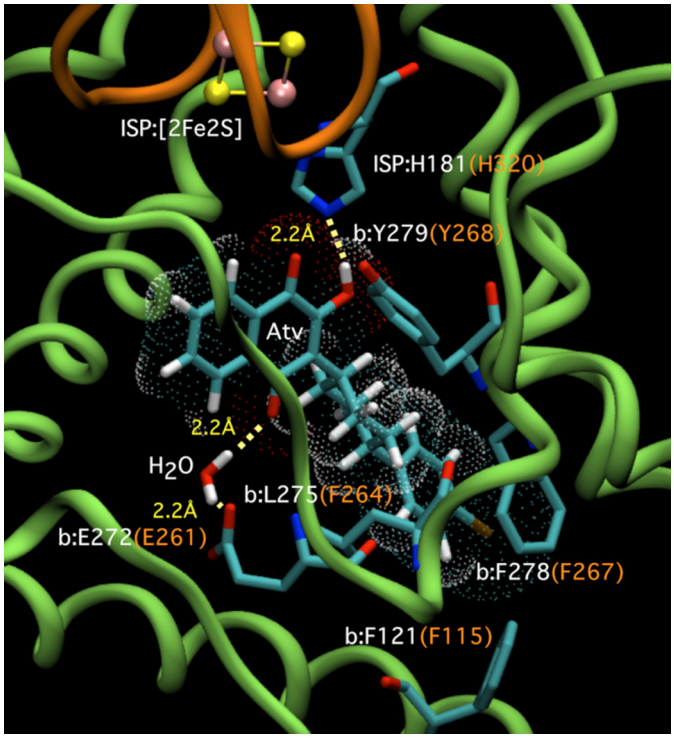

FIGURE 6. **Molecular model of atovaquone (*Atv*) docked into the Q_o site of yeast cytochrome bc_1 complex (Protein Data Bank code 3CX5), showing hydrogen bonding to Rieske protein residue His^{181} and cytochrome *b* residue Glu^{272} (via a bridging water molecule).** Yeast residues are labeled in *white*, with the corresponding *P. falciparum* residues labeled in *orange*. Docking was performed as described under "Experimental Procedures." The cytochrome *b* polypeptide backbone is represented in *green*, with the Rieske protein backbone in *brown*. The [2Fe-2S] cluster of the Rieske protein is represented in CPK form (sulfur, *yellow*; iron, *pink*). Hydrogen bonds are indicated by *yellow dotted lines*. A 1.4 Å radius CPK dotted surface has been added around the docked atovaquone molecule to aid visual clarity. The side chain of His^{181} is shown in the imidazolate conformation, although it has not been established which group contributes the hydrogen atom in the putative hydrogen bond between this residue and the (ionizable) naphthoquinone hydroxyl of atovaquone (10).

study. IC_{50} values were derived from growth inhibition data for the *Plasmodium* strains employed in this investigation and not against the isolated bc_1 complex. Importantly, the introduction of an 8-methyl substituent to the hydroxynapthoquinone moiety was found to counter the resistance conferred by the Y268S mutation in TM90C2B (IC_{50} = 200 nM in blood stage parasite growth assay for compound NQ2). Molecular modeling studies with the yeast bc_1 complex suggested that this methyl substituent would form a van der Waals interaction with the Rieske protein residue Cys^{180}. However, mutation of this conserved residue in yeast resulted in a fully assembled but nonfunctional bc_1 complex (41).

In contrast to our steady-state bc_1 inhibition data with TM90C2B membrane extracts in the presence of atovaquone (Table 2), Hughes *et al.* (40) observed biphasic inhibition titration behavior with the hydroxy-naphthquinones against atovaquone-resistant mutants of the yeast bc_1 complex (*i.e.* incomplete inhibition of activity at an inhibitor concentration of 500 nM) and suggest that the sensitivity of the enzyme to these compounds is dependent on the redox status of the Rieske protein, as is observed for the inhibitor undecyl-hydroxy-benzoxythiazole (42). Although we did not observe a similar biphasic inhibition phenomenon in the current study with atovaquone, it is possible that sensitivity to the redox state of the ISP may be a contributing factor in the 20-fold difference observed in IC_{50} for atovaquone in TM90C2B growth assays and crude bc_1 assays and that this redox state changes on cell disruption.

We predict that the reduced enzyme turnover and the significant reduction in ISP content in parasite bc_1 carrying the Y268S results in a significant fitness cost to the parasite. In line with this hypothesis, a fitness cost (manifested as a slower growth rate) has been demonstrated for atovaquone-resistant K1 clones of *P. falciparum* containing the M133I/G280D double mutation within cytochrome *b* (43).

Analysis of the gene expression of the major metabolic and respiratory chain genes from the TM90C2B strain revealed significant differences in comparison with the 3D7 atovaquone-sensitive strain. In particular key, differences were observed in gene expression of Complex III and Complex IV genes (which included cytochromes *b*, *c*, and c_1, the ISP subunit and subunits 1 and 2 of cytochrome *c* oxidase (Fig. 6)), as well genes involved in glycolysis such as the hexose transporter and phosphoglycerate kinase. It is tempting to speculate therefore that these increased levels of gene expression help the parasite to accommodate the Y268S mutation. The increased levels of Complex III and IV genes may be able to offset the stability issues described above. Mutation of the bc_1 complex in yeast has been shown to have a deleterious effect on the succinate:decylubiquinone oxidoreductase and cytochrome *c* oxidase activity of Complexes II and IV, respectively, which may be due to the disruption of physical associations between these enzymes (37, 38, 44). The increase in expression levels of genes such as the hexose transporter may ameliorate energy deficits. Similarly, induction of the *HXT16* (hexose permease) and *TDH1* (glyceraldehyde-3-phosphate dehydrogenase) genes have been observed in response to treatment of yeast cells with the bc_1 inhibitor myxothiazol (45). *Plasmodium* gene expression has been described as "just in time" expression displaying an S-shaped wave of transcripts (46, 47) and as such is "hard-wired" and largely unresponsive to drug perturbation (48). We assume therefore that the increased levels of gene expression in the TM902CB strain arose from natural variation and were selected by drug pressure.

In summary, this study gives the first description of the effect of the Y268S mutation on parasite bc_1 catalytic turnover and stability. Our data indicate that the reduced enzyme activity affects protein stability and should incur a fitness penalty to the parasite, features that were not fully discernable using the yeast model alone. Gene expression analyses show increased levels of

FIGURE 5. **Fold changes in gene expression of energy metabolism genes between wild type (3D7), transgenic (3D7-yDHODH·GFP), and atovaquone-resistant (TM90C2B) *P. falciparum* parasites.** The figure shows the relative fold change in gene expression for 3D7-yDHODH·GFP/3D7 (*a*) and for TM90C2B/3D7 (*b*). Expression data are normalized against a reference gene (elongation factor 1α) and displayed as mean fold changes ± S.D. from $n \geq 3$ independent experiments. The mean expression data ± S.D. ($n \geq 3$) is shown in supplemental Table S2. The *dashed blue box* indicates genes encoding for components of mitochondrial Complex III and IV.

expression of relevant respiratory chain complexes in parasites harboring the Y268S mutation. It is hypothesized that the increased levels of expression of these key genes offsets the fitness cost of the Y268S mutation to sustain parasite viability.

Acknowledgments—We thank Prof. Dennis Kyle (College of Public Health, University of South Florida) for supplying the atovaquone-resistant isolate TM90C2B (Thailand) and Prof. Akhil Vaidya (Drexel University College of Medicine, Philadelphia, PA) for supplying purified pHHyDHOD-GFP plasmid. We also thank the staff and patients of Ward 7Y and the Gastroenterology Unit of the Royal Liverpool Hospital for the generous donation of blood.

REFERENCES

1. Osei-Akoto, A., Orton, L. C., and Owusu-Ofori, S. (2009) *The Cochrane Database of Systemic Reviews* 2005 **CD004529,** 1–53
2. Painter, H. J., Morrisey, J. M., Mather, M. W., and Vaidya, A. B. (2007) Specific role of mitochondrial electron transport in blood-stage *Plasmodium falciparum*. *Nature* **446,** 88–91
3. Lalloo, D. G., and Hill, D. R. (2008) Preventing malaria in travellers. *BMJ* **336,** 1362–1366
4. Fry, M., and Pudney, M. (1992) Site of action of the antimalarial hydroxynaphthoquinone, 2-[trans-4-(4′-chlorophenyl) cyclohexyl]-3-hydroxy-1,4-naphthoquinone (566C80). *Biochem. Pharmacol.* **43,** 1545–1553
5. Srivastava, I. K., Rottenberg, H., and Vaidya, A. B. (1997) Atovaquone, a broad spectrum antiparasitic drug, collapses mitochondrial membrane potential in a malarial parasite. *J. Biol. Chem.* **272,** 3961–3966
6. Biagini, G. A., Viriyavejakul, P., O'Neill P, M., Bray, P. G., and Ward, S. A. (2006) Functional characterization and target validation of alternative complex I of *Plasmodium falciparum* mitochondria. *Antimicrob. Agents Chemother.* **50,** 1841–1851
7. Hammond, D. J., Burchell, J. R., and Pudney, M. (1985) Inhibition of pyrimidine biosynthesis de novo in *Plasmodium falciparum* by 2-(4-*t*-butylcyclohexyl)-3-hydroxy-1,4-naphthoquinone in vitro. *Mol. Biochem. Parasitol.* **14,** 97–109
8. Seymour, K. K., Yeo, A. E., Rieckmann, K. H., and Christopherson, R. I. (1997) dCTP levels are maintained in *Plasmodium falciparum* subjected to pyrimidine deficiency or excess. *Ann. Trop. Med. Parasitol.* **91,** 603–609
9. Bulusu, V., Jayaraman, V., and Balaram, H. (2011) Metabolic fate of fumarate, a side product of the purine salvage pathway in the intraerythrocytic stages of *Plasmodium falciparum*. *J. Biol. Chem.* **286,** 9236–9245
10. Kessl, J. J., Meshnick, S. R., and Trumpower, B. L. (2007) Modeling the molecular basis of atovaquone resistance in parasites and pathogenic fungi. *Trends Parasitol.* **23,** 494–501
11. Barton, V., Fisher, N., Biagini, G. A., Ward, S. A., and O'Neill, P. M. (2010) Inhibiting *Plasmodium* cytochrome bc_1. A complex issue. *Curr. Opin. Chem. Biol.* **14,** 440–446
12. Korsinczky, M., Chen, N., Kotecka, B., Saul, A., Rieckmann, K., and Cheng, Q. (2000) Mutations in *Plasmodium falciparum* cytochrome *b* that are associated with atovaquone resistance are located at a putative drug-binding site. *Antimicrob. Agents Chemother.* **44,** 2100–2108
13. Musset, L., Bouchaud, O., Matheron, S., Massias, L., and Le Bras, J. (2006) Clinical atovaquone-proguanil resistance of *Plasmodium falciparum* associated with cytochrome *b* codon 268 mutations. *Microbes Infect.* **8,** 2599–2604
14. Berry, A., Senescau, A., Lelièvre, J., Benoit-Vical, F., Fabre, R., Marchou, B., and Magnaval, J. F. (2006) Prevalence of *Plasmodium falciparum* cytochrome *b* gene mutations in isolates imported from Africa, and implications for atovaquone resistance. *Trans. R. Soc. Trop. Med. Hyg.* **100,** 986–988
15. Fisher, N., and Meunier, B. (2008) Molecular basis of resistance to cytochrome bc_1 inhibitors. *FEMS Yeast Res.* **8,** 183–192
16. Fivelman, Q. L., Butcher, G. A., Adagu, I. S., Warhurst, D. C., and Pasvol, G. (2002) Malarone treatment failure and *in vitro* confirmation of resistance of *Plasmodium falciparum* isolate from Lagos, Nigeria. *Malar J.* **1,** 1
17. Schwartz, E., Bujanover, S., and Kain, K. C. (2003) Genetic confirmation of atovaquone-proguanil-resistant *Plasmodium falciparum* malaria acquired by a nonimmune traveler to East Africa. *Clin. Infect. Dis.* **37,** 450–451
18. Fisher, N., and Meunier, B. (2005) Re-examination of inhibitor resistance conferred by Qo-site mutations in cytochrome *b* using yeast as a model system. *Pest Manag. Sci.* **61,** 973–978
19. Wenz, T., Covian, R., Hellwig, P., Macmillan, F., Meunier, B., Trumpower, B. L., and Hunte, C. (2007) Mutational analysis of cytochrome *b* at the ubiquinol oxidation site of yeast complex III. *J. Biol. Chem.* **282,** 3977–3988
20. Biagini, G. A., Fisher, N., Berry, N., Stocks, P. A., Meunier, B., Williams, D. P., Bonar-Law, R., Bray, P. G., Owen, A., O'Neill, P. M., and Ward, S. A. (2008) Acridinediones. Selective and potent inhibitors of the malaria parasite mitochondrial bc_1 complex. *Mol. Pharmacol.* **73,** 1347–1355
21. Trager, W., and Jensen, J. B. (1976) Human malaria parasites in continuous culture. *Science* **193,** 673–675
22. Lambros, C., and Vanderberg, J. P. (1979) Synchronization of *Plasmodium falciparum* erythrocytic stages in culture. *J. Parasitol.* **65,** 418–420
23. Smilkstein, M., Sriwilaijaroen, N., Kelly, J. X., Wilairat, P., and Riscoe, M. (2004) Simple and inexpensive fluorescence-based technique for high-throughput antimalarial drug screening. *Antimicrob. Agents Chemother.* **48,** 1803–1806
24. Looareesuwan, S., Viravan, C., Webster, H. K., Kyle, D. E., Hutchinson, D. B., and Canfield, C. J. (1996) Clinical studies of atovaquone, alone or in combination with other antimalarial drugs, for treatment of acute uncomplicated malaria in Thailand. *Am. J. Trop. Med. Hyg.* **54,** 62–66
25. Kuboyama, M., Yong, F. C., and King, T. E. (1972) Studies on cytochrome oxidase. 8. Preparation and some properties of cardiac cytochrome oxidase. *J. Biol. Chem.* **247,** 6375–6383
26. Fisher, N., Castleden, C. K., Bourges, I., Brasseur, G., Dujardin, G., and Meunier, B. (2004) Human disease-related mutations in cytochrome *b* studied in yeast. *J. Biol. Chem.* **279,** 12951–12958
27. Dechering, K. J., Kaan, A. M., Mbacham, W., Wirth, D. F., Eling, W., Konings, R. N., and Stunnenberg, H. G. (1999) Isolation and functional characterization of two distinct sexual-stage-specific promoters of the human malaria parasite *Plasmodium falciparum*. *Mol. Cell Biol.* **19,** 967–978
28. Knapp, B., Hundt, E., and Küpper, H. A. (1990) *Plasmodium falciparum* aldolase. Gene structure and localization. *Mol. Biochem. Parasitol.* **40,** 1–12
29. Solmaz, S. R., and Hunte, C. (2008) Structure of complex III with bound cytochrome *c* in reduced state and definition of a minimal core interface for electron transfer. *J. Biol. Chem.* **283,** 17542–17549
30. Cheng, Y., and Prusoff, W. H. (1973) Relationship between the inhibition constant (K1) and the concentration of inhibitor which causes 50 per cent inhibition (I50) of an enzymatic reaction. *Biochem. Pharmacol.* **22,** 3099–3108
31. Kessl, J. J., Ha, K. H., Merritt, A. K., Lange, B. B., Hill, P., Meunier, B., Meshnick, S. R., and Trumpower, B. L. (2005) Cytochrome *b* mutations that modify the ubiquinol-binding pocket of the cytochrome bc_1 complex and confer anti-malarial drug resistance in *Saccharomyces cerevisiae*. *J. Biol. Chem.* **280,** 17142–17148
32. Palsdottir, H., Lojero, C. G., Trumpower, B. L., and Hunte, C. (2003) Structure of the yeast cytochrome bc_1 complex with a hydroxyquinone anion Qo site inhibitor bound. *J. Biol. Chem.* **278,** 31303–31311
33. Crofts, A. R., Guergova-Kuras, M., Kuras, R., Ugulava, N., Li, J., and Hong, S. (2000) Proton-coupled electron transfer at the Q_o site. What type of mechanism can account for the high activation barrier? *Biochim. Biophys. Acta* **1459,** 456–466
34. Berry, E. A., and Huang, L. S. (2011) Conformationally linked interaction in the cytochrome bc_1 complex between inhibitors of the Q_o site and the Rieske iron-sulfur protein. *Biochim. Biophys. Acta* **1807,** 1349–1363
35. Wibrand, F., Ravn, K., Schwartz, M., Rosenberg, T., Horn, N., and Vissing, J. (2001) Multisystem disorder associated with a missense mutation in the mitochondrial cytochrome *b* gene. *Ann. Neurol.* **50,** 540–543

36. Covian, R., and Trumpower, B. L. (2006) Regulatory interactions between ubiquinol oxidation and ubiquinone reduction sites in the dimeric cytochrome bc_1 complex. *J. Biol. Chem.* **281,** 30925–30932
37. Brasseur, G., Di Rago, J. P., Slonimski, P. P., and Lemesle-Meunier, D. (2001) Analysis of suppressor mutation reveals long distance interactions in the bc_1 complex of *Saccharomyces cerevisiae*. *Biochim. Biophys. Acta* **1506,** 89–102
38. Brasseur, G., Lemesle-Meunier, D., Reinaud, F., and Meunier, B. (2004) QO site deficiency can be compensated by extragenic mutations in the hinge region of the iron-sulfur protein in the bc_1 complex of *Saccharomyces cerevisiae*. *J. Biol. Chem.* **279,** 24203–24211
39. Cross, R. M., Maignan, J. R., Mutka, T. S., Luong, L., Sargent, J., Kyle, D. E., and Manetsch, R. (2011) Optimization of 1,2,3,4-tetrahydroacridin-9(10H)-ones as antimalarials utilizing structure-activity and structure-property relationships. *J. Med. Chem.* **54,** 4399–4426
40. Hughes, L. M., Lanteri, C. A., O'Neil, M. T., Johnson, J. D., Gribble, G. W., and Trumpower, B. L. (2011) Design of anti-parasitic and anti-fungal hydroxy-naphthoquinones that are less susceptible to drug resistance. *Mol. Biochem. Parasitol.* **177,** 12–19
41. Merbitz-Zahradnik, T., Zwicker, K., Nett, J. H., Link, T. A., and Trumpower, B. L. (2003) Elimination of the disulfide bridge in the Rieske iron-sulfur protein allows assembly of the [2Fe-2S] cluster into the Rieske protein but damages the ubiquinol oxidation site in the cytochrome bc_1 complex. *Biochemistry* **42,** 13637–13645
42. Bowyer, J. R., Edwards, C. A., Ohnishi, T., and Trumpower, B. L. (1982) An analogue of ubiquinone which inhibits respiration by binding to the iron-sulfur protein of the cytochrome bc_1 segment of the mitochondrial respiratory chain. *J. Biol. Chem.* **257,** 8321–8330
43. Peters, J. M., Chen, N., Gatton, M., Korsinczky, M., Fowler, E. V., Manzetti, S., Saul, A., and Cheng, Q. (2002) Mutations in cytochrome b resulting in atovaquone resistance are associated with loss of fitness in *Plasmodium falciparum*. *Antimicrob. Agents Chemother.* **46,** 2435–2441
44. Acín-Pérez, R., Fernández-Silva, P., Peleato, M. L., Pérez-Martos, A., and Enriquez, J. A. (2008) Respiratory active mitochondrial supercomplexes. *Mol. Cell* **32,** 529–539
45. Bourges, I., Horan, S., and Meunier, B. (2005) Effect of inhibition of the bc_1 complex on gene expression profile in yeast. *J. Biol. Chem.* **280,** 29743–29749
46. Bozdech, Z., Llinás, M., Pulliam, B. L., Wong, E. D., Zhu, J., and DeRisi, J. L. (2003) The transcriptome of the intraerythrocytic developmental cycle of *Plasmodium falciparum*. *PLoS Biol.* **1,** E5
47. Le Roch, K. G., Zhou, Y., Blair, P. L., Grainger, M., Moch, J. K., Haynes, J. D., De La Vega, P., Holder, A. A., Batalov, S., Carucci, D. J., and Winzeler, E. A. (2003) Discovery of gene function by expression profiling of the malaria parasite life cycle. *Science* **301,** 1503–1508
48. Ganesan, K., Ponmee, N., Jiang, L., Fowble, J. W., White, J., Kamchonwongpaisan, S., Yuthavong, Y., Wilairat, P., and Rathod, P. K. (2008) A genetically hard-wired metabolic transcriptome in *Plasmodium falciparum* fails to mount protective responses to lethal antifolates. *PLoS Pathog.* **4,** e1000214